

Exploring multimessenger signals from heavy dark matter decay with EDGES 21-cm result and IceCube

Ashadul Halder*

*Department of Physics, St. Xavier's College,
30, Mother Teresa Sarani, Kolkata-700016, India.*

Madhurima Pandey†

*Astroparticle Physics and Cosmology Division,
Saha Institute of Nuclear Physics, HBNI
1/AF Bidhannagar, Kolkata-700064, India.*

Debasish Majumdar‡

*Astroparticle Physics and Cosmology Division,
Saha Institute of Nuclear Physics, HBNI
1/AF Bidhannagar, Kolkata-700064, India*

Rupa Basu§

*Department of Physics, St. Xavier's College,
30, Mother Teresa Sarani, Kolkata-700016, India*

(Dated: February 25, 2022)

Abstract

The primordial heavy or superheavy dark matter that could be created during the reheating or preheating stage of the Universe can undergo QCD cascade decay process to produce leptons or gamma as end products. Although these could be rare decays, the energy involved in such decay process can influence 21cm signal of hyperfine transition of neutral hydrogen during the reionization era. We explore in this work, possible multimessenger signals of such heavy dark matter decays. One of which could be the source of ultra high energy neutrino (of \sim PeV energy regime) signals at IceCube detector whereas the other signal attributes to the cooling/heating of the baryons by the exchange of energy involved in this decay process and its consequent influence on 21cm signal. The effect of evaporation of primordial black holes and baryon scattering with light cold dark matter are also included in relation to the 21cm signal temperature and their influence are also discussed.

Keywords: 21-cm; heavy dark matter; dark matter decay; dark matter - baryon; primordial black hole

I. INTRODUCTION

The dynamics of the Universe in the dark age is still unexplored due to the lack of luminous sources. The 21-cm neutral hydrogen spectrum can be a promising probe in understanding the dynamics of the early Universe particularly during this unexplored era. The redshifted signature of the 21-cm hydrogen absorption spectrum may provide a detailed understanding regarding the reionization and the Primordial Black Holes (PBHs) [1{9] as well as the baryon-dark matter (DM) scattering and neutrino physics [10] in the high redshifted epoch.

Keeping this in view, we explore in this work possible multimessenger signals from possible rare decay of fundamental heavy dark matter. Heavy dark matter of mass as high as 10^8 GeV or more could be created via gravitational production mechanism, non-linear quantum effects during the reheating or preheating stages after inflation. These dark matters are therefore produced non-thermally in the early Universe and are long lived. Thus these heavy or super heavy dark matter, it exists exhibits rare decay. These heavy or super heavy dark

* ashadul.halder@gmail.com

† madhurima.pandey@saha.ac.in

‡ debasish.majumdar@saha.ac.in

§ rupabasu.in@gmail.com

matter may undergo decay via QCD cascades. The primary products qq , on hadronization and decay produce leptons, γ etc. as the end products. Ultra high energy (UHE) neutrinos could be one of the final products of this decay process. We alternate these UHE neutrinos from the decay of primordial heavy dark matter to be the source of UHE ν signal at IceCube neutrino detection of \sim PeV energy regime. On the other hand, we also explore the energy involved in this decay process and the influence of the heating effect on the evolution of absorption temperature of 21-cm hydrogen line during the reionization era. In doing so, we have included other heating/cooling effects in this regard that could have been caused by the collisions of cold dark matter particles with baryons and the evaporation of primordial black holes or PBH.

The neutrino events at the IceCube neutrino detector are an important probe to the sources for UHE neutrinos. The high energy starting event (HESE) data of IceCube for neutrinos with energies > 20 TeV indicate a power law spectrum for IceCube neutrinos. We conclude here 7.5 year IceCube HESE data for neutrino signal in the energy range 2×10^5 to 4×10^6 GeV and assume them to be the neutrino signal of heavy dark matter decay discussed above.

The "Experiment to Detect the Global Epoch of Reionization Signature" (EDGES) [11] reported a prominent footprint of 21-cm line (21cm brightness temperature -500_{-500}^{+200} mK) at cosmic dawn ($14 < z < 20$) with 99% confidence level (C.L.). But according to the notion of the standard cosmology, the estimated brightness temperature is only ≈ -200 mK. As a consequence, the additional cooling observed by the EDGES experiment can be explained either by enhancing the background temperature T_γ or by lowering the baryonic temperature which is almost equal to the spin temperature at $14 < z < 20$. The evaporation of primordial black holes (PBHs) can be such a possible source that heats up the intergalactic medium (IGM) resulting in the rise in background temperature. Dark matter annihilation, decay and even the baryon-dark matter interaction could be the possible sources that can induce the larger than the expected separation between T_s and T_γ [12-14]. In the present work, we address the effects of possible decay of heavy dark matter or HDM on the 21-cm absorption temperature signal. In addition, the influence of PBH evaporation and the baryon-DM interactions are also included in a single framework to study the 21-cm absorption temperature and its evolution.

The hydrogen atom has two hyperfine electronic ground states namely a singlet spin 0

and a triplet spin 1. The transition from the higher energy triplet state to the lower energy singlet produces the 21-cm radio spectrum which is described by the brightness temperature T_{21} . The expression of the brightness temperature at different redshift z is given by,

$$T_{21} = \frac{T_s - T_\gamma}{1 + z} (1 - e^{-\tau(z)}) \quad (1)$$

where, T_s is the spin temperature at redshift z and $\tau(z)$ is the optical depth of the medium, given by [15],

$$\tau(z) = \frac{3}{32\pi} \frac{T_\star}{T_s} n_{\text{HI}} \lambda_{21}^3 \frac{A_{10}}{H(z) + (1+z)\delta_r v_r}. \quad (2)$$

In the above expression (Eq. 2) $T_\star (= hc/k_B \lambda_{21} = 0.068 \text{ K})$, $A_{10} = 2.85 \times 10^{-15} \text{ s}^{-1}$ is the Einstein coefficient [16, 17], $\lambda_{21} \approx 21 \text{ cm}$ and $\delta_r v_r$ is the radial gradient of the peculiar velocity.

The spin temperature (T_s) is characterized as,

$$\frac{n_1}{n_0} = 3 \exp -\frac{T_\star}{T_s}, \quad (3)$$

where n_0 and n_1 are the number densities of neutral hydrogen atoms at singlet spin-0 and triplet spin-1 state respectively. The resonant scattering of Ly α photons and the background photons mainly modify the spin temperature. On the other hand, the combined effect of HDM decay, Hawking radiation and baryon-DM scattering also modify T_s remarkably. The expression of T_s as function of cosmic microwave background (CMB) temperature T_γ ($T_\gamma = 2.725(1+z) \text{ K}$) and baryon temperature T_b is given by,

$$T_s = \frac{T_\gamma + y_c T_b + y_{\text{Ly}\alpha} T_{\text{Ly}\alpha}}{1 + y_c + y_{\text{Ly}\alpha}}, \quad (4)$$

where, the term $y_{\text{Ly}\alpha}$ arises due to the Wouthuysen-Field effect. $T_{\text{Ly}\alpha}$ and y_c are the Lyman- α background temperature and the collisional coupling parameter respectively [2]. The coefficients y_c and $y_{\text{Ly}\alpha}$ are given by $y_c = \frac{C_{10} T_\star}{A_{10} T_b}$ and $y_{\text{Ly}\alpha} = \frac{P_{10} T_\star}{A_{10} T_{\text{Ly}\alpha}} e^{0.3 \times (1+z)^{1/2} T_b^{-2/3} \left(1 + \frac{0.4}{T_b}\right)^{-1}}$ [3, 18, 19]. Here, P_{10} is the deexcitation rate due to Ly α given by $P_{10} \approx 1.3 \times 10^{-21} S_\alpha J_{-21} \text{ s}^{-1}$ where C_{10} is the collision deexcitation rate, S_α is the spectral distortion factor [20] and J_{-21} represents the Lyman- α background intensity [21].

Energy injection is also possible in case of the decay of heavy primordial dark matter. Such dark matter can be gravitationally produced in the early Universe or it can also be produced during the reheating phase after inflation. Such a heavy dark matter can undergo cascading decay processes through hadronic or leptonic (or both) to produce ultra high

energy (UHE) neutrinos (and other particles). The UHE neutrinos can be detected by Km^2 detectors such as IceCube. IceCube has detected neutrinos in the PeV energy range. Such possibilities are earlier explored in Ref. [22].

In this work, we study possible multimessenger signals of heavy dark matter whereby the two effects namely the neutrinos from heavy dark matter decay and the possible effects on 21-cm signal at reionization epoch due to the heat transfer following the decay process are addressed. In the present work, we consider two additional effects on the evolution of baryon temperature T_b , while computing the temperature of the T_{21} line at dark ages and reionization epoch. One is the heavy dark matter decay and the other is the evaporation of primordial black holes or PBHs. In addition, the effect of the dark matter - baryon collision in the evolution of T_b are also included.

Throughout the calculation, the baryon-DM interaction cross-section (σ) is parameterized as $\sigma = \sigma_0 v^{-4}$ [15], where the lighter dark matter is considered to be model-independent [23{29]. In the case of PBH heating, only the effect of the Hawking radiation is taken into account. It is to be mentioned that, in this work, we consider two types of dark matter. One is a dark matter in the mass range of hundreds of MeV to few GeV, that interacts with baryons and affects temperature T_{21} of 21-cm line, while the other is a heavy dark matter that may have been produced after the inflationary epoch and can undergo cascading decay to produce leptons and injects energy into the system. The latter also can influence T_{21} , while the former accounts for almost all the dark matter in the Universe, the fraction of heavy dark matter is negligibly small.

The paper is organized as follows. Section II describes the heavy dark matter decay and production of PeV neutrinos. Here IceCube neutrinos are assumed to be originated from heavy dark matter decay. In Section III, the formalism for the evolution of baryon temperature T_b and dark matter temperature T_χ are described. Here both the effects of heavy dark matter decay and PBH evaporation are considered. The results and corresponding plots are described in Section IV. Finally, in Section V, the concluding remarks are given.

II. HEAVY DARK MATTER DECAY

The decay of heavy dark matter (HDM) having mass significantly higher than the electroweak scale takes place via the cascading of QCD partons [30{33]. We used only the

hadronic decay channel ($\chi \rightarrow qq$) in our calculation as the contribution of the leptonic decay channel ($\chi \rightarrow ll$) is much smaller than the hadronic channel [22, 30]. The total spectrum at scale $s = M_{\text{HDM}}^2$ can be obtained by summing over all Parton fragmentation function $D^h(x, s)$ from the decay of particle h . Here $x = \frac{2E}{M_{\text{HDM}}}$ is the dimensionless energy. In our current analysis, only muon decay is considered in this calculation as the total contribution of the other mesons is negligible ($< 10\%$) [30, 32].

The spectra of neutrinos (ν), photons (γ) and electrons (e) are written as [30],

$$\frac{dN_\nu}{dx} = 2R \int_{xR}^1 \frac{dy}{y} D^{\pi^\pm}(y) + 2 \int_x^1 \frac{dz}{z} f_{\nu_i} \left(\frac{y}{z} \right) D^{\pi^\pm}(z), \quad (5)$$

$$\frac{dN_\gamma}{dx} = 2 \int_x^1 \frac{dz}{z} D^{\pi^0}(z), \quad (6)$$

$$\frac{dN_e}{dx} = 2R \int_x^1 \frac{dy}{y} \left(\frac{5}{3} + 3y^2 + \frac{4}{3}y^3 \right) \int_{x/y}^{x/(ry)} \frac{dz}{z} D^{\pi^\pm}(z). \quad (7)$$

In the above equations (Eqs. 5, 6 and 7), we can define $D^\pi(x, s)$ as $D^\pi \equiv [D_q^\pi(x, s) + D_g^\pi(x, s)]$, where $x = \frac{2E}{M_{\text{HDM}}}$ and $R = \frac{1}{1-r}$, where $r = (m_\mu/m_\pi)^2 \approx 0.573$. The functions $f_{\nu_i}(x)$ are adopted from Ref. [34]

$$\begin{aligned} f_{\nu_i}(x) &= g_{\nu_i}(x) (x-r) + (h_{\nu_i}^{(1)}(x) + h_{\nu_i}^{(2)}(x)) (r-x), \\ g_{\nu_\mu}(x) &= \frac{3-2r}{9(1-r)^2} (9x^2 - 6 \ln x - 4x^3 - 5), \\ h_{\nu_\mu}^{(1)}(x) &= \frac{3-2r}{9(1-r)^2} (9r^2 - 6 \ln r - 4r^3 - 5), \\ h_{\nu_\mu}^{(2)}(x) &= \frac{(1+2r)(r-x)}{9r^2} [9(r+x) - 4(r^2 + rx + x^2)], \\ g_{\nu_e}(x) &= \frac{2}{3(1-r)^2} [(1-x)(6(1-x)^2 + r(5+5x-4x^2)) + 6r \ln x], \\ h_{\nu_e}^{(1)}(x) &= \frac{2}{3(1-r)^2} [(1-r)(6-7r+11r^2-4r^3) + 6r \ln r], \\ h_{\nu_e}^{(2)}(x) &= \frac{2(r-x)}{3r^2} (7r^2 - 4r^3 + 7xr - 4xr^2 - 2x^2 - 4x^2r). \end{aligned} \quad (8)$$

In this work, the neutrinos, photons and electrons spectra are obtained by computing Eqs. 5, 6 and 7 respectively for different values of M_{HDM} . The neutrino spectrum $\frac{dN_\nu}{dx}$ in Eq. 5 represents the combination of neutrinos and antineutrinos spectrum of all three flavours (ν_e , ν_μ and ν_τ) where the neutrinos are considered to be produced from pion decay in ratio 1:2:0 at the source. Similarly, for the case of electron spectrum ($\frac{dN_e}{dx}$), Eq. 7 denotes the combined spectrum of electrons and positrons.

The extragalactic counterpart of heavy dark matter decaying muon neutrino flux is given by,

$$\frac{d_{\text{EG}}}{dE}(E_\nu) = \frac{\mathcal{K}}{4\pi M_{\text{HDM}}} \int_0^\infty \frac{\rho_0 c/H_0}{\sqrt{\Omega_m(1+z^3) + (1-\Omega_m)}} \frac{dN_{\nu_\mu}}{dE}[E(1+z)]dz. \quad (9)$$

In the above equation (Eq. 9), $\mathcal{K} = f_{\text{HDM}}$ and the hubble radius (the proper radius of the hubble sphere) is given as c/H_0 , where $c/H_0 = 1.37 \times 10^{28}$ cm. The average dark matter density of the Universe at $z = 0$ (the present epoch) is denoted as $\rho_0 (= 1.15 \times 10^{-6} \text{ GeV/cm}^3)$ and $\Omega_m = 0.316$ where Ω_m represents the contribution of the matter density normalized to the critical density of the Universe. The neutrinos oscillate from one flavour to another during their propagation from the source to Earth. But given the astronomical distance they traverse before reaching the Earth, the neutrinos originated with a flavour ratio $\nu_e : \nu_\mu : \nu_\tau = 1 : 2 : 0$ (as the oscillation part is averaged out) and reaches the Earth with a flavour ratio $1 : 1 : 1$. Thus the muon neutrino spectrum $\frac{dN_{\nu_\mu}}{dE} = \frac{1}{3} \frac{dN_\nu}{dE}$ on reaching the Earth.

In addition to the extragalactic part, the galactic ν_μ flux from similar decay is given by

$$\frac{d_{\text{G}}}{dE}(E_\nu) = \frac{\mathcal{K}}{4\pi M_{\text{HDM}}} \int_V \frac{\rho_\chi(R[r])}{4\pi r^2} \frac{dN_{\nu_\mu}}{dE}(E, l, b) dV, \quad (10)$$

where l and b denote the Galactic coordinates. The density of dark matter at distance R from the Galactic centre (GC) is denoted as $\rho_\chi(R[r])$ and r is the distance from the Earth. In our calculation, we have taken into account the Navarro-Frenk-White (NFW) profile for the dark matter density and the integration is performed over the Milky Way halo for which R_{max} is considered to be 260 Kpc.

The total flux, which is also referred to as the total theoretical flux (ϕ^{Th}), at energy E_ν can be obtained by considering the contribution of both the galactic and the extragalactic ν_μ flux as

$$\phi^{\text{Th}}(E_\nu) = \frac{d_{\text{EG}}}{dE}(E_\nu) + \frac{d_{\text{G}}}{dE}(E_\nu). \quad (11)$$

We perform a χ^2 fit of the IceCube results (7.5 yr IceCube HESE data [35]) for PeV neutrinos with the present formalism of heavy dark matter decay and obtain mass and \mathcal{K} of the decaying dark matter. The χ^2 is defined as

$$\chi^2 = \frac{1}{n} \sum_{i=1}^n \left(\frac{E_i^2 \phi_i^{\text{Th}} - E_i^2 \phi_i^{\text{Ex}}}{(\text{err})_i} \right)^2, \quad (12)$$

where the number of chosen points are $n (= 4)$ and E_i represent the energy corresponding to data point i . In Eq. 12, $(\text{err})_i$ is the error of the i^{th} chosen experimental point. The

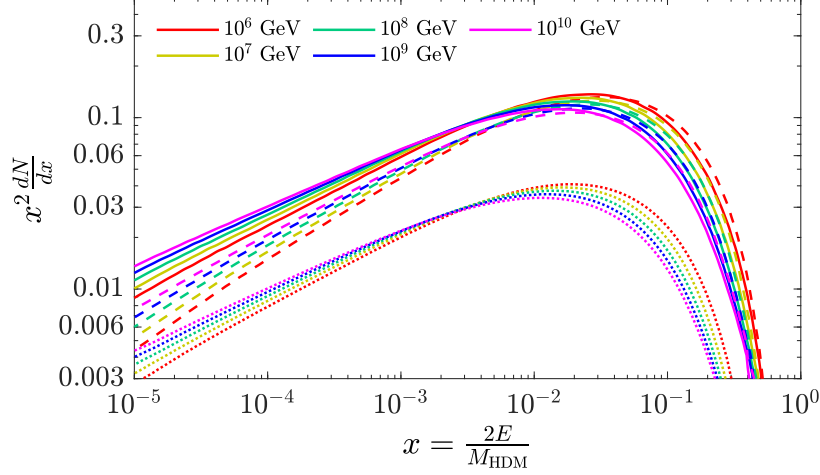


FIG. 1. Spectra of heavy dark matter decay for different dark matter masses. The solid lines represent the total neutrino spectra ($\nu_e + \nu_\mu + \nu_\tau$, $\nu + \bar{\nu}$) for different M_{HDM} . The corresponding γ and e spectra are described by dashed and dotted lines respectively.

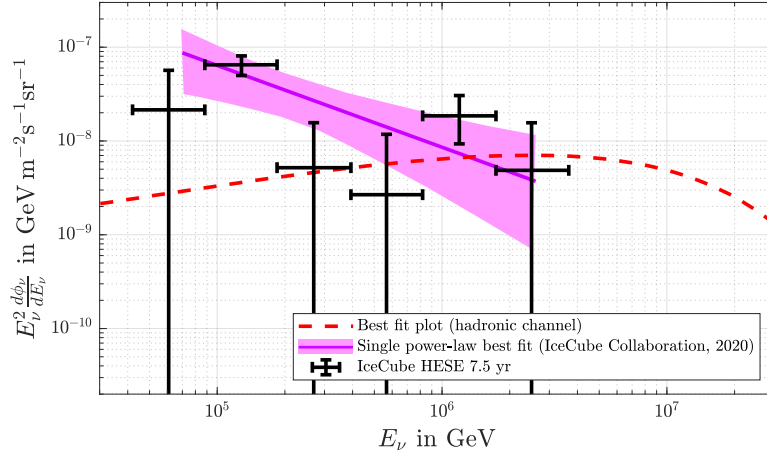


FIG. 2. Bestfit ν_μ spectrum from heavy dark matter decay.

superscripts Th and Ex correspond to the theoretical (calculated) and experimental (observed) flux respectively. For this two-parameter χ^2 fit, we consider only the hadronic decay channel as the contribution due to the leptonic decay channel for the chosen four data points is negligible [22]. From the analysis, the obtained best fit values of HDM mass (M_{HDM}) and \mathcal{K} are $M_{\text{HDM}} = 2.754 \times 10^8 \text{ GeV}$ and $\mathcal{K} = 2.5556 \times 10^{-29} \text{ sec}^{-1}$ respectively. In Fig. 2, six observed data points (two points in the energy range 60-120 TeV and four data points in the PeV energy range ($2 \times 10^5 \sim 4 \times 10^6 \text{ GeV}$)) with error bars are plotted. In our

calculation, we consider the last four data points observed by IceCube in and around PeV energy range. The red dashed line in Fig. 2 indicates the calculated ν_μ flux for the best fit values of M_{HDM} and \mathcal{K} . Moreover, we also estimate best fit values of \mathcal{K} for different HDM masses (see Fig. 3).

III. TEMPERATURE EVOLUTION

In our analysis, the thermal evolution of the charge-neutral Universe ($x_e = x_p$, where x_e and x_p are the abundances of the electron and proton respectively) is studied by evolving the dark matter temperature (T_χ) and the baryon temperature (T_b) with cosmological redshift z . After incorporating the effects of energy injection from PBH evaporation and the baryon-DM interaction, the evolution equations (T_χ and T_b of Ref. [15]) take the form [2, 3, 15, 36, 37],

$$(1+z) \frac{dT_\chi}{dz} = 2T_\chi - \frac{2Q_\chi}{3H(z)}, \quad (13)$$

$$(1+z) \frac{dT_b}{dz} = 2T_b + \frac{c}{H(z)}(T_b - T_\gamma) - \frac{2Q_b}{3H(z)} - \frac{2}{3k_B H(z)} \frac{K_{\text{BH}} + K_{\text{HDM}}}{1 + f_{\text{He}} + x_e}, \quad (14)$$

where c is the rate of Compton interaction, given by $c = \frac{8\sigma_T a_r T_\gamma^4 x_e}{3(1+f_{\text{He}}+x_e)m_e c}$. σ_r and a_T are the radiation constant and the Thomson scattering cross-section respectively and x_e and f_{He} are the fractional abundance of electron and He. The last term of the Eq. 14 represents additional contributions to the evolution of baryon temperature T_b due to heavy dark matter decay [2, 38] and PBH evaporation [2, 3, 37]. The quantities K_{BH} and K_{HDM} are defined in Eq. 18. The baryon-DM fluid (Q_b and Q_χ) interaction depends on the drag term $V_{\chi b}$ [15]. The evolution of $V_{\chi b}$ is described as [15],

$$\frac{dV_{\chi b}}{dz} = \frac{V_{\chi b}}{1+z} + \frac{1}{(1+z)H(z)} \frac{\rho_m \sigma_0}{m_b + m_\chi} \frac{1}{V_{\chi b}^2} F(r), \quad (15)$$

where, $F(r) = \text{erf}(r/\sqrt{2}) - \sqrt{2/\pi} r e^{-r^2/2}$ (erf represents the error function), $r = V_{\chi b}/u_{\text{th}}$ and $\sigma_{41} = \frac{\sigma_0}{10^{-41} \text{cm}^2}$. The term u_{th}^2 is the variance of the relative thermal motion.

The free electron abundance x_e of the Universe also depends significantly on the amount of energy deposited in the medium. The variation of the electron abundance x_e with redshift z given by [3, 15, 37],

$$\frac{dx_e}{dz} = \frac{1}{(1+z)H(z)} [I_{\text{Re}}(z) - I_{\text{Ion}}(z) - (I_{\text{BH}}(z) + I_{\text{HDM}}(z))], \quad (16)$$

where, $I_{\text{Re}}(z)$ is the the standard recombination and $I_{\text{Ion}}(z)$ is the ionization rate respectively [15{17, 37, 39}. As both terms ($I_{\text{Re}}(z)$ and $I_{\text{Ion}}(z)$) are functions of T_b and T_γ [5, 17, 37, 39{43], the term x_e depends on baryon temperature and DM temperature simultaneously.

The term I_{src} (src=BH, HDM) appears in the expression of electron abundance evolution (Eq. 16) is described as

$$I_{\text{src}} = \chi_i f(z) \frac{1}{n_b} \frac{1}{E_0} \times \left. \frac{dE}{dV dt} \right|_{\text{src}}. \quad (17)$$

The term K_{src} (src=BH or HDM) in Eq. 14 is given by,

$$K_{\text{src}} = \chi_h f(z) \frac{1}{n_b} \times \left. \frac{dE}{dV dt} \right|_{\text{src}}. \quad (18)$$

where E_0 is the amplitude of the ground state energy of hydrogen atom, $\chi_i = (1 - x_e)/3$ and $\chi_h = (1 + 2x_e)/3$ are the fractions of the energy deposited in the form of ionization and heating respectively [3, 4, 44{46]. In Eqs. 17 and 18, the parameter $f(z)$ is the ratio of total amount of energy deposited to the injected energy [36, 47{50]. In the case of HDM decay, the term $f(z)$ is estimated by incorporating the photon and electron spectra as obtained by the Eqs. 6 and 7 (see section II) [36, 47{50]. At higher redshift and energy, almost entire flux of electrons transfer to photons by the process of inverse Compton scatter (ICS) and above the threshold of pair-production, the photons efficiently produce e^-e^+ pair. Those electrons and positrons will rapidly reduce to low energy e^- and e^+ via ICS and cascade. As a consequence, in the calculation of $f(z)$, the transfer function does not change significantly with increasing DM mass at higher values. Moreover, it can be noticed that, the available grid data of energy transfer function [47, 48] is almost constant for $\gtrsim 10^3$ GeV for fixed values of input and output redshift [36, 47{50]. So, in the case of HDM with different masses, we use the transfer function for $10^{12.75}$ eV in our calculations (the electron and photon spectrum are estimated from Eqs. 6 and 7 of Section II).

It is to be noted that two categories of dark matter are considered in this work. One is the heavy dark matter produced in the early Universe, the decay of which inject energy into the system and produce UHE neutrinos, while the other is the usual WIMP dark matter that scatters with baryons and exchange heat. Both the processes influence the temperature of the 21-cm line.

In the case of PBH evaporation, the radiation contains several particle species [51]. But the contribution of electron and photon emissions are most relevant in the case of energy depositions in the gas medium [2]. The rate of the energy injection due to Hawking radiation

is written as [2, 37],

$$\left. \frac{dE}{dVdt} \right|_{\text{BH}} = \sum_{i=\gamma, e^\pm} \mathcal{F}_i \frac{dM_{\text{BH}}}{dt} n_{\text{BH}}(z) \quad (19)$$

where, $n_{\text{BH}}(z)$ is the PBH number density at redshift z , and is given by [3],

$$\begin{aligned} n_{\text{BH}}(z) &= \beta_{\text{BH}} \left(\frac{1+z}{1+z_{\text{eq}}} \right)^3 \frac{\rho_{\text{c,eq}}}{\mathcal{M}_{\text{BH}}} \left(\frac{\mathcal{M}_{\text{H,eq}}}{\mathcal{M}_{\text{H}}} \right)^{1/2} \left(\frac{g_\star^i}{g_\star^{\text{eq}}} \right)^{1/12} \\ &\approx 1.46 \times 10^{-4} \beta_{\text{BH}} (1+z)^3 \left(\frac{\mathcal{M}_{\text{BH}}}{\text{g}} \right)^{-3/2} \text{cm}^{-3} \end{aligned} \quad (20)$$

In the above, \mathcal{M}_{BH} is the mass of the PBH at the time of formation and \mathcal{M}_{H} is the horizon mass [3, 52, 53]. The quantity β_{BH} represents the initial mass fraction of PBHs.

A black hole of mass M_{BH} evaporates at the rate [2, 54]

$$\frac{dM_{\text{BH}}}{dt} \approx -5.34 \times 10^{25} \left(\sum_i \mathcal{F}_i \right) M_{\text{BH}}^{-2} \text{g/sec} \quad (21)$$

where the coefficient \mathcal{F}_i represents the evaporation fraction in the form of i^{th} particle. The energy injection due to the HDM decay is given by,

$$\left. \frac{dE}{dVdt} \right|_{\text{HDM}} = \rho_\chi f_{\text{HDM}} \quad , \quad (22)$$

where f_{HDM} is the fraction of dark matter in the form of heavy dark matter and Γ_{HDM} is the width of HDM decay. In the present work, we introduce a new parameter $\mathcal{K} = f_{\text{HDM}} \Gamma_{\text{HDM}}$. With this, Eq. 22 takes the form, $\left. \frac{dE}{dVdt} \right|_{\text{HDM}} = \rho_\chi \mathcal{K}$.

IV. CALCULATIONS AND RESULTS

As mentioned earlier, in the present work, we explore the possible multimessenger effect due to heavy dark matter decay in the framework of global 21-cm signature, where the effects of PBH evaporation and the baryon-DM interaction have also been included. Two categories of dark matter are considered here. One is the possible decay of heavy dark matter to produce ultra high energy neutrinos and their detection by IceCube, while the other is a WIMP type cold dark matter (CDM) interaction strength in the weak interaction regime. We assume that the fraction of DM in the form of HDM is very small in comparison to that of the lighter CDM type dark matter. From Eqs. 14, 18, 22, it can be seen that the decay of heavy dark matter (and the PBH evaporation) contributes to the evolution of

baryon temperature T_b and consequently the 21-cm absorption temperature T_{21} . Also the heavy dark matter cascading decay can produce UHE neutrinos that could be detected by km² detector such as IceCube. Here in this work, the best fit values for heavy dark matter decay width (in fact $\mathcal{K} = f_{\text{HDM}}$) is further constrained for different possible HDM masses M_{HDM} in case of different m_χ values. by the EDGES result for 21-cm absorption line. While computing T_{21} , in addition to the effects of heavy dark matter decay, the collisional effects of baryons with CDM (that is assumed to account for almost all the dark matter in the Universe), the evaporation of primary black holes etc. By performing this analysis we also attempted to explore the contribution of a very small fraction of heavy dark matter through its decay and the contribution of the overwhelming CDM type dark matter through their collisional effects with baryon in presence PBH evaporation contributes to 21-cm Hydrogen absorption line during reionization era. As mentioned, various constraints are estimated using the experimental results of the EDGES experiment ($T_{21} = -500^{+200}_{-500}$ at $z = 17.2$). The brightness temperature at redshift $z = 17.2$ is a important quantity in this analysis, represented by T_{21} .

We simultaneously solve computationally Eqs. 13, 14, 15, 16, 17, 18, 19, 20, 21, 22 and obtain the baryon temperature. The spin temperature is then computed using Eq. 4 where the effect of Ly α forest are also included. Finally T_{21} is calculated using Eqs. 1, 2. In Fig. 3, the allowed regions in the \mathcal{K} - M_{HDM} parameter plane are shown for different chosen values of DM mass m_χ . The four plots in Fig. 3 corresponds to (a) $m_\chi = 0.3$ GeV, (b) $m_\chi = 0.38$ GeV, (c) $m_\chi = 0.4$ GeV and (d) $m_\chi = 1.0$ GeV. The allowed region is estimated using the experimental excess of EDGES. The uppermost line of the shaded region (upper dashed black line) corresponds to $T_{21} = -300$ mK while the lower black dashed line corresponds to $T_{21} = -1000$ mK. The values of T_{21} at any points between the upper and lower limits are indicated by the corresponding colour code (see colour bar). In the case of $m_\chi = 0.3$ GeV, the permissible zone lie far above the best fit points, which are obtained from the χ^2 analysis using the IceCube HESE 7.5 yr data. However, comparing the plots of Fig. 3a, 3b, 3c and 3d we see that, as m_χ increases, the lower bound falls rapidly, while the upper bound decreases gradually and for $m_\chi \gtrsim 0.4$ GeV, IceCube best fit lie in the allowed region, which is obtained using the observational excess of EDGES. For all the cases, the values of PBH parameters are chosen to be $\mathcal{M}_{\text{BH}} = 10^{14}$ g and $\beta_{\text{BH}} = 10^{29}$, while σ_{41} is fixed at 1.

We also address bounds in the m_χ - σ_{41} space for different values of PBH masses (\mathcal{M}_{BH}) for

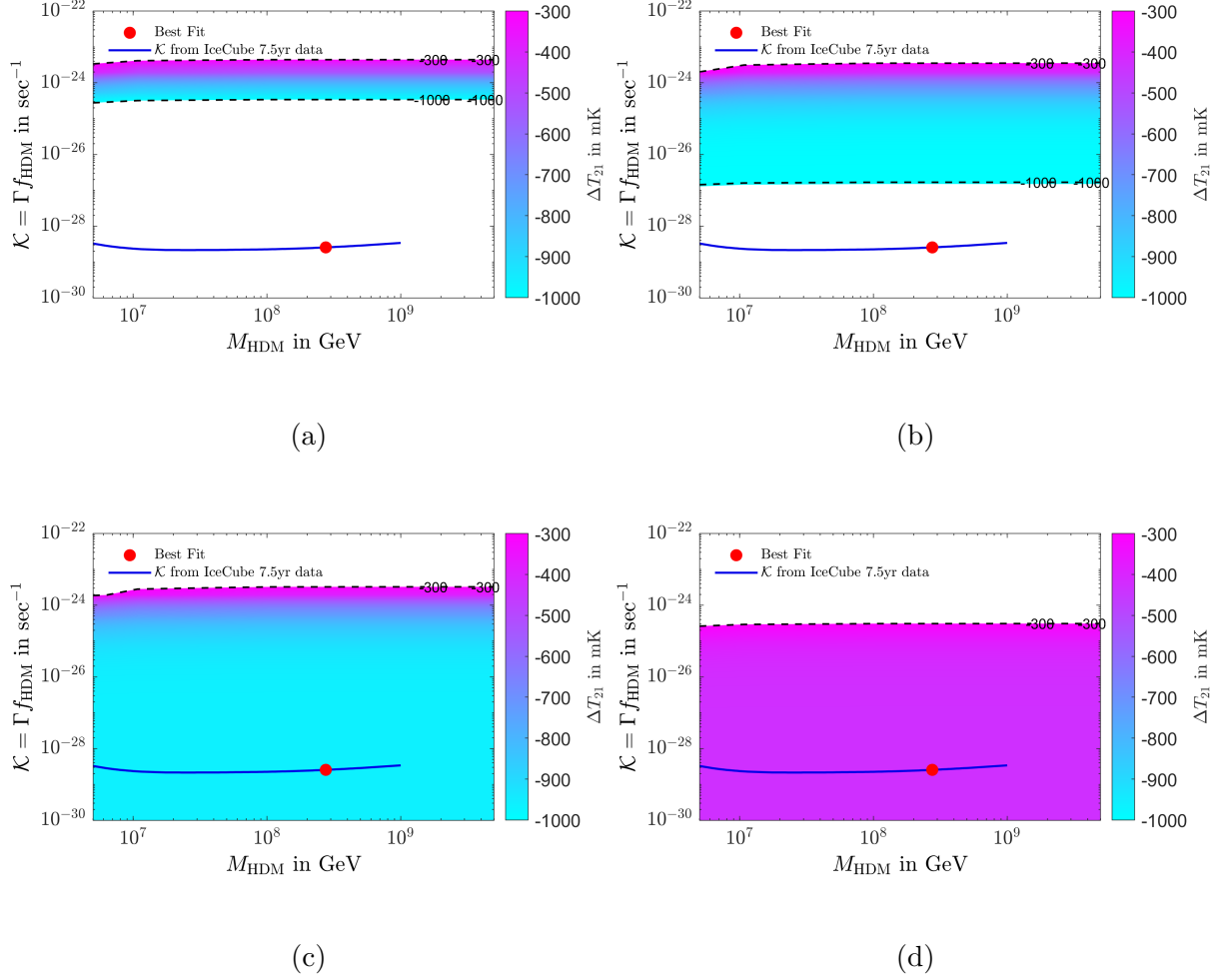


FIG. 3. The allowed zone in the \mathcal{K} - M_{HDM} plane for (a) $m_\chi = 0.3$ GeV, (b) $m_\chi = 0.38$ GeV, (c) $m_\chi = 0.4$ GeV and (d) $m_\chi = 1.0$ GeV, where other variables are kept fixed at $\sigma_{41} = 1$, $\mathcal{M}_{\text{BH}} = 10^{14}\text{g}$ and $\beta_{\text{BH}} = 10^{29}$. The upper and lower bounds are correspond to the $\Delta T_{21} = -300$ mK and -1000 mK respectively. The solid blue line indicates bestfit values of \mathcal{K} for different values of M_{HDM} (from IceCube HESE 7.5yr data), while the red dot symbol specifies the bestfit \mathcal{K} for bestfit M_{HDM} .

the best fit values of M_{HDM} and \mathcal{K} (obtained from IceCube results). The results are shown in Fig. 4. In Fig. 4, the area between the solid and dashed lines (of the same colour) represents the allowed range in the m_χ - σ_{41} space. It can be seen that as the value of \mathcal{M}_{BH} decreases upto around 10^{14}g , the allowed zone shifts toward lower values of m_χ and higher values of σ_{41} (for $\mathcal{M}_{\text{BH}} \lesssim 10^{14}\text{g}$). But in the case when $\mathcal{M}_{\text{BH}} = 0.6 \times 10^{14}\text{g}$, the σ_{41} - m_χ allowed region appears to shift to higher m_χ - lower σ_{41} domain. We fixed that this shift of m_χ - σ_{41} allowed

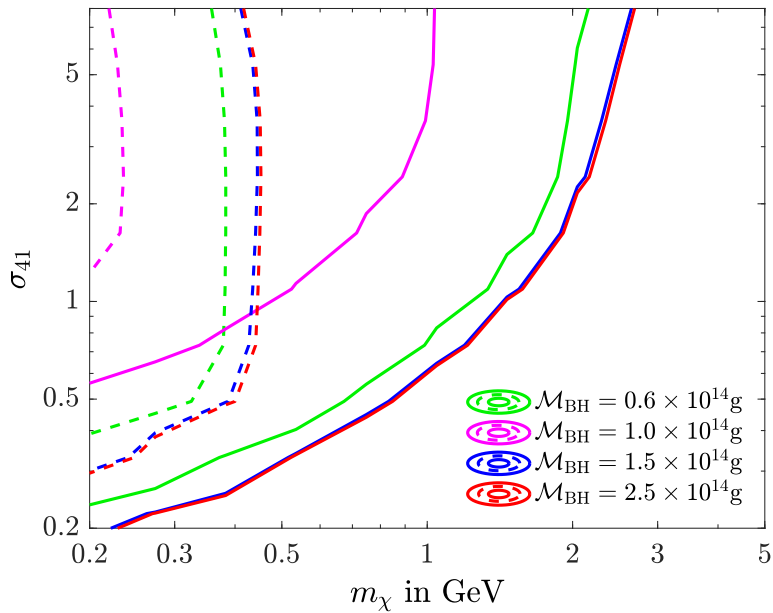


FIG. 4. The allowed region in the $\sigma_{41} - m_\chi$ parameter plane for different PBH masses where, the chosen values of M_{HDM} and \mathcal{K} are the bestfit values, obtained from the χ^2 analysis using the IceCube 7.5 year data [35]. The different coloured solid lines are addressing the bound corresponds to $\Delta T_{21} = -300$ mK for different PBH masses while the dashed lines are representing the same for $\Delta T_{21} = -1000$ mK. Consequently, in each case, the region between the solid and the corresponding dashed line (of individual colour) indicates the allowed zone in the m_χ - σ_{41} plane.

zone in the opposite direction sets in for $\mathcal{M}_{\text{BH}} \lesssim 0.8 \times 10^{14}$ g. For PBH mass $\sim 0.6 \times 10^{14}$ g (4), the black holes evaporate very early. Therefore such PBHs are unable to heat up the baryonic fluid significantly. As a consequence, in this particular case, the allowed region is close to those for higher values of \mathcal{M}_{BH} . In all four cases, the β_{BH} is chosen to be 10^{-29} . It is to be noted that, for the best fit values of M_{HDM} and \mathcal{K} , the maximum possible value of the m_χ is $2 \sim 3$ GeV, when the energy injection by PBH is comparatively low and agree with the results of Barkana [55] (i.e. $m_\chi \leq 3$ GeV).

V. SUMMARY AND DISCUSSIONS

In this work, two possible multimessenger signals from the decay of a heavy dark matter are addressed. One is the neutrino signals (of \sim PeV energies) from rare decays of such

heavy dark matter at IceCube neutrino experiment and the other is the influence of this decay process on the absorption temperature of 21-cm Hydrogen signal.

A heavy or super heavy dark matter { non-thermal particle candidates { can be produced in the very early Universe, after the inflationary phase during preheating or reheating era or during the GUT phase [56{62]. They may be produced from nonlinear quantum effects, as consequence of inflation decays or by gravitational production mechanisms. These long lived particles can undergo rare decays to produce leptons as the end product. Such decays of super heavy dark matter proceed via QCD parton cascades and these are discussed in Ref. [30{33, 63{65]. The decay cascades are addressed using Dokshitzer-Grivov-Lipatov-Altarelli-Parisi equations or DGLAP equations in short. The electroweak radiative corrections can also be incorporated into the numerical evolution of DGLAP equations. In the hadronic channel of the decay via QCD cascades, the heavy or super heavy dark matter first decays to qq which then hadronizes to produce leptons and/or γ s as the final products. In this work, the numerical evolutions and Monte Carlo simulations are performed to obtain the spectrum of neutrinos as the end product of the decay cascade of the heavy dark matter of a given mass. We have verified that the neutrino spectrum obtained from the leptonic decay channels via electroweak cascade is not very useful and relevant for the PeV neutrino energy window of IceCube results. Hence is not included in the present calculations.

On the other hand, the brightness temperature (T_{21}) of 21-cm radio signal of hydrogen depends on the spin temperature T_s , the matter temperature or baryon temperature T_b (T_b and T_s are coupled and at some epoch are same) and the background temperature T_γ . The EDGES experiment has measured T_{21} during the era of reionization at the redshift region $14 < z < 20$ with the central value of $z \sim 17.2$. The T_{21} results along with its 99% C.L. (-500^{+200}_{-500} mK) values appear to be cooler than the value of $T_{21} \sim -200$ mK calculated from the astrophysical and cosmological consideration at the same redshift. With T_γ , the cosmic background radiation temperature, the temperature T_s is influenced or modified by the processes that inject or absorb heat from the system. This can be thought to happen by possible collisions of dark matter with the baryons, the effects of Ly α forest etc. or other processes through which the baryons can be heated up or cooled down. In this work, we have also included and studied the effects of the evaporations of primordial black holes or PBHs on the evolution of T_b . It is found that the mass m_χ of the dark matter that collides with the baryon and affects the baryon temperature (and hence T_{21}) should be in the range

of hundreds of MeV to few GeV (around upto 2-3 GeV for PBH mass of $\sim 10^{14}$ g). These dark matter particles are thermally produced and their interaction strength is in the weak interaction regime and are assumed to account for the dark matter relic abundance of the Universe. The fraction of heavy dark matter whose rare decay is addressed in this work related to multimessenger study is considered to be very small. The multimessenger study is performed with respect to the possible effects on T_{21} of the rare decay of primordial heavy dark matter. To this end, in this work, the heat exchange due to the process that heavy dark decaying to neutrinos are also included in the evolution equation of T_b .

With this motivation, the neutrino spectrum from a primordial heavy dark matter decay is first computed and then compared with the IceCube neutrino signal. For this purpose, 7.5 year of IceCube data are chosen in the neutrino energy window of 2×10^5 GeV to 4×10^6 GeV. It contains four data points. The calculated neutrino spectrum is then fitted with the IceCube results and the best fit value of mass and decay width (the product \mathcal{K} of decay width and the density fraction) of the heavy dark matter are obtained. The other possible multimessenger signal from the heavy dark matter decay in relation to its influence on T_{21} signal is addressed by including the effect of this decay in the formalism for computing T_{21} temperature. To this end, the effect of heavy dark matter decay has been included in the evolution equation of baryon temperature. In addition, the evaporation effects of primordial black holes via Hawking radiation and baryon-dark matter (low mass dark matter as mentioned above) collision are also incorporated and T_{21} is computed at various redshift values. The EDGES observational results for T_{21} are then used to constrain the $\mathcal{K} - M_{\text{HDM}}$ plane. It is found that both the multimessenger signals considered for heavy dark matter decay signal, namely the IceCube PeV neutrinos and T_{21} temperature are satisfied when the dark matter mass m_χ (with which the baryons in the early Universe collide to influence T_{21} signal) is $m_\chi \geq 0.4$ GeV and PBH mass $\mathcal{M}_{\text{BH}} \approx 10^{14}$ GeV.

In addition, we also explore how the mass of PBH affects the dark matter-baryon scattering cross-section (σ_{41}) for different possible dark matter masses (m_χ) of few GeV in presence of heavy dark matter decay contributions to T_{21} . To this end, we use T_{21} results and constrain $\sigma_{41} - m_\chi$ plane. The heavy dark matter mass M_{BH} and decay width \mathcal{K} are kept fixed at their best fit values ($M_{\text{BH}} = 2.754 \times 10^8$ GeV, $\mathcal{K} = 2.5556 \times 10^{-29}$ sec $^{-1}$) obtained from the analysis of IceCube 7.5 year HESE data. We find $m_\chi < 3$ GeV in order to satisfy the EDGES results for $\mathcal{M}_{\text{BH}} \leq 2.5 \times 10^{14}$ g.

Thus this work is a detailed multimessenger study of the possible heavy dark matter decay signals with IceCube 7.5 year data and 21-cm absorption line temperature of hydrogen and EDGES results, while simultaneously exploring the effects of Ly α forest and PBH evaporation on 21 cm signal.

ACKNOWLEDGEMENTS

First we would like to thank Tracy Slatyer for his suggestion and help in the calculation of energy deposition. Two of the authors (A.H. and R.B.) wish to acknowledge the support received from St. Xavier's College, Kolkata. One of the authors (A.H.) also thanks the University Grant Commission (UGC) of the Government of India, for providing financial support. One of the authors (MP) thanks the DST-INSPIRE fellowship (DST/INSPIRE/FELLOWSHIP/IF160004) grant by DST, Govt. of India. One of the authors (R.B.) also thanks the Women Scientist Scheme-A fellowship (SR/WOS-A/PM-49/2018), Department of Science & Technology (DST), Govt. of India, for providing financial support.

-
- [1] O. Mena, S. Palomares-Ruiz, P. Villanueva-Domingo, and S. J. Witte, Constraining the primordial black hole abundance with 21-cm cosmology, *Phys. Rev. D* **100**, 043540 (2019).
 - [2] S. J. Clark, B. Dutta, Y. Gao, Y.-Z. Ma, and L. E. Strigari, 21 cm limits on decaying dark matter and primordial black holes, *Phys. Rev. D* **98**, 043006 (2018).
 - [3] Y. Yang, Constraints on primordial black holes and curvature perturbations from the global 21-cm signal, *Phys. Rev. D* **102**, 083538 (2020).
 - [4] K. J. Mack and D. H. Wesley, Primordial black holes in the dark ages: Observational prospects for future 21cm surveys (2008), arXiv:0805.1531 [astro-ph].
 - [5] K. L. Pandey and A. Mangalam, Role of primordial black holes in the direct collapse scenario of supermassive black hole formation at high redshifts, *Journal of Astrophysics and Astronomy* **39**, 9 (2018).
 - [6] A. Hektor, G. Hütsi, L. Marzola, M. Raidal, V. Vaskonen, and H. Veermäe, Constraining Primordial Black Holes with the EDGES 21-cm Absorption Signal, *Phys. Rev. D* **98**, 023503

- (2018), arXiv:1803.09697 [astro-ph.CO].
- [7] P. Villanueva-Domingo, O. Mena, and S. Palomares-Ruiz, A brief review on primordial black holes as dark matter, *Frontiers in Astronomy and Space Sciences* **8**, 87 (2021).
- [8] P. Villanueva-Domingo and K. Ichiki, 21 cm Forest Constraints on Primordial Black Holes, (2021), arXiv:2104.10695 [astro-ph.CO].
- [9] H. Zhou, Z. Li, H. Gao, and Z. Huang, Constraints on the abundance of primordial black holes with different mass distributions from lensing of fast radio bursts, (2021), arXiv:2103.08510 [astro-ph.CO].
- [10] M. Chianese, P. Di Bari, K. Farrag, and R. Samanta, Probing relic neutrino radiative decays with 21cm cosmology, *Physics Letters B* **790**, 64 (2019).
- [11] J. D. Bowman, A. E. E. Rogers, R. A. Monsalve, T. J. Mozdzen, and N. Mahesh, An absorption profile centred at 78 megahertz in the sky-averaged spectrum, *Nature* **555**, 67 (2018).
- [12] R. Basu, S. Banerjee, M. Pandey, and D. Majumdar, Lower bounds on dark matter annihilation cross-sections by studying the fluctuations of 21-cm line with dark matter candidate in inert doublet model (idm) with the combined effects of dark matter scattering and annihilation (2020), arXiv:2010.11007 [astro-ph.CO].
- [13] A. Hektor, G. Hütsi, L. Marzola, and V. Vaskonen, Constraints on ALPs and excited dark matter from the EDGES 21-cm absorption signal, *Phys. Lett. B* **785**, 429 (2018), arXiv:1805.09319 [hep-ph].
- [14] A. Chatterjee, P. Dayal, T. R. Choudhury, and A. Hutter, Ruling out 3 keV warm dark matter using 21 cm EDGES data, *Mon. Not. Roy. Astron. Soc.* **487**, 3560 (2019), arXiv:1902.09562 [astro-ph.CO].
- [15] J. B. Muñoz, E. D. Kovetz, and Y. Ali-Haïmoud, Heating of baryons due to scattering with dark matter during the dark ages, *Phys. Rev. D* **92**, 083528 (2015).
- [16] Y. Ali-Haïmoud and C. M. Hirata, Ultrafast effective multilevel atom method for primordial hydrogen recombination, *Phys. Rev. D* **82**, 063521 (2010).
- [17] Y. Ali-Haïmoud and C. M. Hirata, Hyrec: A fast and highly accurate primordial hydrogen and helium recombination code, *Phys. Rev. D* **83**, 043513 (2011).
- [18] Q. Yuan, B. Yue, X.-J. Bi, X. Chen, and X. Zhang, Leptonic dark matter annihilation in the evolving universe: constraints and implications, *Journal of Cosmology and Astroparticle Physics* **2010** (10), 023.

- [19] M. Kuhlen, P. Madau, and R. Montgomery, The spin temperature and 21 cm brightness of the intergalactic medium in the pre-reionization era, *The Astrophysical Journal* **637**, L1 (2006).
- [20] C. M. Hirata, Wouthuysen-Field coupling strength and application to high-redshift 21-cm radiation, *Monthly Notices of the Royal Astronomical Society* **367**, 259 (2006).
- [21] B. Ciardi and P. Madau, Probing beyond the epoch of hydrogen reionization with 21 centimeter radiation, *The Astrophysical Journal* **596**, 1 (2003).
- [22] M. Pandey, D. Majumdar, A. Halder, and S. Banerjee, Mass and life time of heavy dark matter decaying into icecube pev neutrinos, *Physics Letters B* **797**, 134910 (2019).
- [23] L. Lopez Honorez and C. E. Yaguna, The inert doublet model of dark matter revisited, *Journal of High Energy Physics* **2010**, 46 (2010).
- [24] S. Banerjee, F. Boudjema, N. Chakrabarty, G. Chalons, and H. Sun, Relic density of dark matter in the inert doublet model beyond leading order: The heavy mass case, *Phys. Rev. D* **100**, 095024 (2019).
- [25] H.-C. Cheng, J. L. Feng, and K. T. Matchev, Kaluza-Klein dark matter, *Phys. Rev. Lett.* **89**, 211301 (2002), arXiv:hep-ph/0207125 [hep-ph].
- [26] G. Servant and T. M. P. Tait, Is the lightest Kaluza-Klein particle a viable dark matter candidate?, *Nucl. Phys.* **B650**, 391 (2003), arXiv:hep-ph/0206071 [hep-ph].
- [27] D. Hooper, G. Zaharijas, D. P. Finkbeiner, and G. Dobler, Prospects For Detecting Dark Matter With GLAST In Light Of The WMAP Haze, *Phys. Rev.* **D77**, 043511 (2008), arXiv:0709.3114 [astro-ph].
- [28] D. Majumdar, Relic densities for Kaluz-Klein dark matter, *Mod. Phys. Lett.* **A18**, 1705 (2003).
- [29] A. Dutta Banik, M. Pandey, D. Majumdar, and A. Biswas, Two component wimp–fimp dark matter model with singlet fermion, scalar and pseudo scalar, *The European Physical Journal C* **77**, 657 (2017).
- [30] M. Kachelrieß, O. E. Kalashev, and M. Y. Kuznetsov, Heavy decaying dark matter and icecube high energy neutrinos, *Phys. Rev. D* **98**, 083016 (2018).
- [31] V. Berezhinsky, M. Kachelrieß, and S. Ostapchenko, Electroweak jet cascading in the decay of superheavy particles, *Phys. Rev. Lett.* **89**, 171802 (2002).
- [32] R. Aloisio, V. Berezhinsky, and M. Kachelriess, Fragmentation functions in supersymmetric qcd and ultrahigh energy cosmic ray spectra produced in top-down models, *Phys. Rev. D* **69**, 094023 (2004).

- [33] V. Berezhinsky and M. Kachelriess, Monte carlo simulation for jet fragmentation in susy qcd, Phys. Rev. D **63**, 034007 (2001).
- [34] S. R. Kelner, F. A. Aharonian, and V. V. Bugayov, Energy spectra of gamma rays, electrons, and neutrinos produced at proton-proton interactions in the very high energy regime, Phys. Rev. D **74**, 034018 (2006).
- [35] R. Abbasi *et al.* (IceCube), The IceCube high-energy starting event sample: Description and flux characterization with 7.5 years of data, (2020), arXiv:2011.03545 [astro-ph.HE].
- [36] S. Galli, T. R. Slatyer, M. Valdes, and F. Iocco, Systematic uncertainties in constraining dark matter annihilation from the cosmic microwave background, Phys. Rev. D **88**, 063502 (2013).
- [37] A. Halder and M. Pandey, Investigating the effect of pbh, dark matter – baryon and dark matter – dark energy interaction on edges in 21cm signal (2021), arXiv:2101.05228 [astro-ph.CO].
- [38] A. Mitridate and A. Podo, Bounds on Dark Matter decay from 21 cm line, JCAP **05**, 069, arXiv:1803.11169 [hep-ph].
- [39] A. Halder and S. Banerjee, Bounds on Abundance of Primordial Black Hole and Dark Matter from EDGES 21cm Signal, (2021), arXiv:2102.00959 [astro-ph.CO].
- [40] P. J. E. Peebles, Recombination of the Primeval Plasma, Astrophysical Journal **153**, 1 (1968).
- [41] D. G. Hummer, Total Recombination and Energy Loss Coefficients for Hydrogenic Ions at Low Density for $10^4 \text{T/E/Z}/2; 10^7 \text{K}$, MNRAS **268**, 109 (1994).
- [42] D. Pequignot, P. Petitjean, and C. Boisson, Total and effective radiative recombination coefficients., A&A **251**, 680 (1991).
- [43] S. Seager, D. D. Sasselov, and D. Scott, A new calculation of the recombination epoch, The Astrophysical Journal **523**, L1 (1999).
- [44] X. Chen and M. Kamionkowski, Particle decays during the cosmic dark ages, Phys. Rev. D **70**, 043502 (2004).
- [45] L. Zhang, X. Chen, M. Kamionkowski, Z.-g. Si, and Z. Zheng, Constraints on radiative dark-matter decay from the cosmic microwave background, Phys. Rev. D **76**, 061301 (2007).
- [46] S. R. Furlanetto, S. P. Oh, and E. Pierpaoli, The Effects of Dark Matter Decay and Annihilation on the High-Redshift 21 cm Background, Phys. Rev. D **74**, 103502 (2006), arXiv:astro-ph/0608385.

- [47] M. S. Madhavacheril, N. Sehgal, and T. R. Slatyer, Current Dark Matter Annihilation Constraints from CMB and Low-Redshift Data, *Phys. Rev. D* **89**, 103508 (2014), arXiv:1310.3815 [astro-ph.CO].
- [48] T. R. Slatyer, Indirect Dark Matter Signatures in the Cosmic Dark Ages II. Ionization, Heating and Photon Production from Arbitrary Energy Injections, *Phys. Rev. D* **93**, 023521 (2016), arXiv:1506.03812 [astro-ph.CO].
- [49] H. Liu, G. W. Ridgway, and T. R. Slatyer, Code package for calculating modified cosmic ionization and thermal histories with dark matter and other exotic energy injections, *Phys. Rev. D* **101**, 023530 (2020), arXiv:1904.09296 [astro-ph.CO].
- [50] S. K. Acharya and R. Khatri, CMB and BBN constraints on evaporating primordial black holes revisited, *JCAP* **06**, 018, arXiv:2002.00898 [astro-ph.CO].
- [51] J. H. MacGibbon, Quark- and gluon-jet emission from primordial black holes. ii. the emission over the black-hole lifetime, *Phys. Rev. D* **44**, 376 (1991).
- [52] Y. Yang, Constraints on the small-scale curvature perturbation using Planck-2015 data, *MNRAS* **486**, 4569 (2019).
- [53] A. S. Josan, A. M. Green, and K. A. Malik, Generalized constraints on the curvature perturbation from primordial black holes, *Phys. Rev. D* **79**, 103520 (2009).
- [54] S. W. HAWKING, Black hole explosions?, *Nature* **248**, 30 (1974).
- [55] R. Barkana, Possible interaction between baryons and dark-matter particles revealed by the first stars, *Nature* **555**, 71 (2018).
- [56] D. J. H. Chung, E. W. Kolb, and A. Riotto, Superheavy dark matter, *Phys. Rev. D* **59**, 023501 (1998).
- [57] V. A. Kuzmin and I. I. Tkachev, Ultrahigh-energy cosmic rays, superheavy long-lived particles, and matter creation after inflation, *Journal of Experimental and Theoretical Physics Letters* **68**, 271 (1998).
- [58] D. J. H. Chung, E. W. Kolb, and A. Riotto, Nonthermal supermassive dark matter, *Phys. Rev. Lett.* **81**, 4048 (1998).
- [59] D. J. H. Chung, E. W. Kolb, and A. Riotto, Production of massive particles during reheating, *Phys. Rev. D* **60**, 063504 (1999).
- [60] D. J. H. Chung, P. Crotty, E. W. Kolb, and A. Riotto, Gravitational production of superheavy dark matter, *Phys. Rev. D* **64**, 043503 (2001).

- [61] G. Gelmini and P. Gondolo, Dm production mechanisms (2010), arXiv:1009.3690 [astro-ph.CO].
- [62] *Particle Dark Matter: Observations, Models and Searches* (Cambridge University Press, 2010).
- [63] C. T. Hill, Monopolonium, Nuclear Physics B **224**, 469 (1983).
- [64] P. Bhattacharjee and G. Sigl, Monopole annihilation and highest energy cosmic rays, Phys. Rev. D **51**, 4079 (1995).
- [65] V. Berezhinsky and A. Vilenkin, Cosmic necklaces and ultrahigh energy cosmic rays, Phys. Rev. Lett. **79**, 5202 (1997).